



## Synthesis, Characterization and Electrical Properties of ZnO Nanoparticles Dispersed in Poly(vinyl acetal)/PVA Composite

ISSAM A. LATIF<sup>1,\*</sup>, HILAL M. ABDULLAH<sup>1</sup>, SUNDUS H. MARZA<sup>1</sup>, AMMAR H. AL-DUJAILI<sup>1</sup> and EMAD T. BAKIR<sup>2</sup>

<sup>1</sup>Department of Chemistry, College of Education, Ibn Al-Haitham, University of Baghdad, Baghdad, Iraq

<sup>2</sup>Department of Chemistry, College of Science, University of Tekrit, Tekrit, Iraq

\*Corresponding author: Fax: +96414251347; Tel: +96 47901394895; E-mail: dr\_issam2003@yahoo.com

(Received: 17 September 2012;

Accepted: 13 July 2013)

AJC-13801

Poly 4-methyl benzylidene vinyl alcohol [poly(vinyl acetal)] was prepared and characterized with IR spectroscopy and the melting point measured, ZnO nanoparticles were prepared and with AFM and XRD characterized, studied and the nanoparticles size measured. Poly (vinyl acetal)/PVA composite were prepared by ultrasonically mixing with different ZnO nanoparticles per cent. Each mixture was fabricated in film and casted in 5 cm × 5 cm glass caste. The real and imaginary dielectric permittivity and electric modulus were for the prepared films studied.

**Key Words:** ZnO nanocomposite, Polymer nanocomposite dielectric constant, ZnO nanoparticles.

### INTRODUCTION

The inorganic nanoparticles doping into the polymer matrix can provide high-performance novel materials that find applications in many industrial fields. As a result of the development in nanotechnology, inorganic nanostructured materials have been designed/discovered and fabricated with important cooperative physical phenomena such as super paramagnetism, size-dependent band-gap, ferromagnetism, electron and phonon transport. Yet, they typically suffer from high manufacture expense and the shaping and further processing of these materials is often difficult and demanding or impossible<sup>1</sup>.

Polymers, on the other hand, are flexible light weight materials and can be produced at a low cost. They are also known to allow easy processing and can be shaped into thin films by various techniques such as dip-coating, spin-coating, film-casting and printing. Polymers are widely used in the optoelectronics industry and are playing important roles in various applications.

Therefore, the drawbacks of using inorganic nanostructured materials can be overcome by employing a polymer matrix to embed a relatively small content of inorganic nanoparticles. The integration of inorganic nanoparticles into a polymer matrix allows both properties from inorganic nanoparticles and polymer to be combined/enhanced and thus advanced new functions can be generated to the polymer-inorganic nanocomposites poly inorganic nanocomposites. The poly inorganic nanocomposites are one kind of composite materials comprising

of nanometer-sized inorganic nanoparticles, typically in the range of 1-100 nm, which are uniformly dispersed in and fixed to a polymer matrix. Nanoparticles filled polymers provide advantages over micron-filled polymers because they provide resistance to degradation<sup>2</sup> and improvement in thermo-mechanical properties without causing a reduction in dielectric strength. The published results for electrical voltage endurance in these new materials indicate that very substantial improvements in voltage endurance can be demonstrated. These improvements in dielectric properties observed for nano-filled polymers could be due to several factors: (i) the large surface area of nanoparticles which creates a large 'interaction zone' or region of altered polymer behaviour<sup>3</sup>, (ii) changes in the polymer morphology due to the surfaces of particles<sup>4</sup>, (iii) a reduction in the internal field caused by the decrease in size of the particles, (iv) changes in the space charge distribution<sup>5,6</sup> and (v) a scattering mechanism. It should also be recognized that this technology also results in characteristic changes in non-electrical properties<sup>7</sup>. In this way, the inorganic nanoparticles are acting like 'additives' to enhance polymer performance and thus are termed as nano-fillers or nano-inclusions<sup>8,9</sup>. Before 20 years, the term 'nanocomposites' was not popular and 'hybrid' or 'molecular composite' were used instead<sup>10</sup>. In that time, inorganic fillers had already been used as additives for polymers to enhance mechanical, thermal and chemical stability. However, traditional fillers were often in micron size and did not possess the superior properties of nanoparticles.

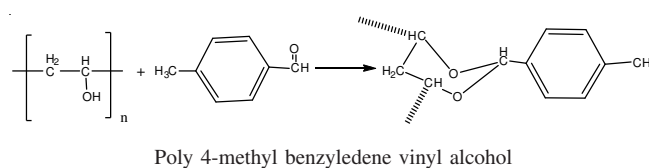
Recently, the polymer inorganic nanocomposites with high dielectric permittivity have been considered to be potential candidates for integration into electronic devices. Owing to the continuous development towards the miniaturization of electronics, newer dielectric materials were sought which would enable to achieve high energy density for capacitor applications. Ceramics possessing high dielectric permittivity are being used as voltage capacitors due to their high breakdown voltages. However, they are brittle, suffer from poor mechanical strength and hence cannot be exposed to high fields. Polymer films such as polyester, polycarbonate, polypropylene, polystyrene, polyethylene sulphide and polyvinyl acetal<sup>11</sup> are being used in the fabrication of low leakage capacitors. Though polymers possess relatively low dielectric permittivity, they can withstand high fields, are flexible and easy to process. By combining the advantages of both, one can fabricate new hybrid materials with high dielectric permittivity and high breakdown voltages to achieve high volume efficiency and energy storage density for applications in capacitors as electric energy storage devices<sup>12-15</sup>. This study aims the achievement of ZnO nanostructures in the reaction temperature of 70 °C by the solochemical method using zinc nitrate hexahydrate and sodium hydroxide. The product obtained was characterized by X-ray diffraction (XRD) technique method. The morphology and size of the ZnO was investigated with AFM and SEM. Among the nanomaterials with industrial relevance stands out zinc oxide, an *n* type semiconductor that displays a hexagonal crystalline Wurtzite-type structure, with space group P63 mc and lattice parameters of  $a = b = 0.3250$  nm and  $c = 0.5207$  nm<sup>16</sup>. The importance of ZnO is due to its unusual physical properties such as high conductance, chemical and thermal stability<sup>17</sup>, wide and direct band gap of 3.37 eV<sup>18</sup> and a high excitation binding energy of 60 M eV<sup>19</sup>. Moreover, it has good radiation resistance<sup>20</sup> and is harmless to the environment<sup>21</sup>. The ZnO nanostructures has great potentiality for being used in preparing solar cell, acoustic, electrical and optical devices, chemical sensors<sup>22</sup>, catalysts, pigments, cosmetics, varistors and gas sensors<sup>23</sup>.

## EXPERIMENTAL

**Synthesis of ZnO nanoparticles:** All the reagents used in this experiment, NaOH and Zn(NO<sub>3</sub>)<sub>2</sub>·6H<sub>2</sub>O, were of analytical grade from Aldrich and were used without any further purification. In two liter beaker NaOH was dissolved in deionized water to a concentration of (1 M, 250 mL) and the resulting solution was heated, under constant stirring, to the temperature of 70 °C. After achieving this temperature, 1 mL from commercial dodecyl sulfate anionic surfactants added and then from a burette the solution of (0.5 M, 100 mL) Zn(NO<sub>3</sub>)<sub>2</sub>·6H<sub>2</sub>O was for 2 h dripped into the 2 L beaker containing the aqueous solution of NaOH under continual stirring. In this procedure the reaction temperature was constantly maintained in 70 °C. The suspension formed with the dropping of 0.5 M Zn(NO<sub>3</sub>)<sub>2</sub>·6H<sub>2</sub>O solution to the alkaline aqueous solution was kept stirred for 2 h at 70 °C. The material formed was filtered and washed several times with deionized water<sup>24</sup>. The washed sample was dried at 65 °C in oven for several hours. The yield of the ZnO nanostructures by this method is *ca.* 92 %. The dry ZnO nanoparticles examined with XRD (Shimadzu XRD-

6000) with copper radiation (CuK<sub>α</sub>, 1.5406 Å), the prepared nanoparticles size and morphology were also observed with atomic force microscopy (AFM) and scanning electron microscope (SEM).

**Synthesis of poly 4-methyl benzylidene vinyl alcohol (poly(vinyl acetal)) compound:** All chemicals used in the preparation are from Sigma-Aldrich. The preparation procedure of poly(vinyl acetal) compound was based on the work of Sakurada<sup>25</sup>. PVA (Mw = 12000 g, 0.5 g) and 4-methyl benzaldehyde (10 mmol, 12 g) was dissolved in mixture of benzene (24 mL) and ethanol (6 mL) with 2 drops of HCl. the reaction mixture was left stirring vigorously at (40-50 °C) for 24 h the solution was poured into excess of methanol (100 mL) containing equimolar amount of NaOH, the product was separated by filtration and then washed with methanol and dried in vacuum. The yield of the product was 80 %.



**Poly 4-methyl benzylidene vinyl alcohol -PVA with ZnO nanocomposites film fabrication:** Four polymer composite films were prepared and the composition percentage are shown in Table-1, each portion dissolved in 20 mL DMF and mixed completely under constant stirring for 1 h while the mixture was heated up till 50 °C then the mixture was let to cool down to room temperature (24 °C) with stirring of the mixture was carried out to ensure a homogenous composition.

TABLE-1  
COMPOSITIONS OF THE PREPARED FILMS

Film No.	Poly(vinyl acetal) (g/film)	PVA (g/film)	ZnO g (%/film)
1	0.166	0.0	0.00
2	0.166	0.2	1.71
3	0.166	0.2	2.81
4	0.166	0.2	3.79

The obtained poly(vinyl acetal)/PVA composition was mixed ultrasonically with ZnO nanoparticles as shown in Table-1 for (15-25) min. To cast the films, the above mixtures were poured in a casting glass plate 5 cm × 5 cm and let it dry at room temperature for 140 h. At the expiry of this time, the films were ready which were peeled off the casting glass plate.

**Dielectric constant measurements:** The above fabricated films were cut into 2 cm × 1.5 cm pieces to fit a homemade silver electrode for characterization by measuring dielectric properties using Precision LCR meter HP 4274 A connected with HP 4275 A and test fixture HP 16047 A at frequency range 100-105 Hz.

## RESULTS AND DISCUSSION

The IR spectrum (Fig. 1) of poly 4-methyl benzylidene vinyl alcohol show an absorption band in the region (3500-3200) cm<sup>-1</sup> due to the stretching vibration of unacetalized (OH) group of (PVA), absorption band at (3050) cm<sup>-1</sup> and at (2950-

2850)  $\text{cm}^{-1}$  attributed to (C-H) aliphatic and aromatic stretching vibration and absorption band in the region (1250-1150)  $\text{cm}^{-1}$  for (C-O-C cyclic ether) stretching vibration. A medium absorption band at (840)  $\text{cm}^{-1}$  attributed to the out of plane bending vibration of 1,4-substituted benzene ring is also appeared. The melting point was 385 °C which investigated with a hot stage polarizing microscope (Olympus BX51M).

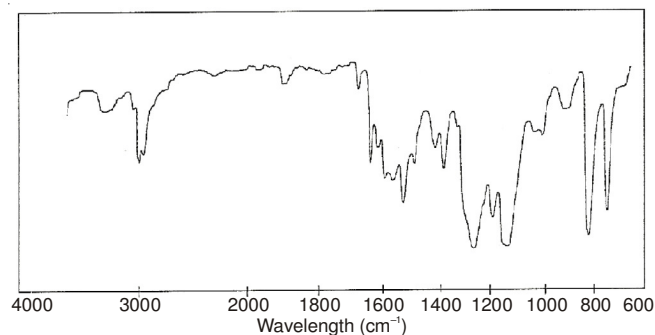


Fig. 1. IR spectrum of poly-4-methyl benzylidene vinyl alcohol

**Atomic force microscope (AFM) and scanning electron microscope (SEM):** The atomic force microscope (AFM) Fig. 2a-b show two and three dimensional histogram, respectively, represent ZnO nanoparticles, their typical diameter was less than (41.7 nm). The particle size histogram was performed and shown the particles which are to a large extent well-separated from one another throughout the field of the micrograph and agreed with SEM micrograph Fig. 2c and show spherical ZnO nanoparticles.

**X-Ray diffraction (XRD):** The XRD spectra of ZnO nanoparticles are shown in Fig. 3, a series of characteristic peaks: 2.8112(100), 2.5996(002), 2.4702(101), 1.9092(102), 1.6239(110), 1.4763(103), 1.4060(200), 1.3777(112) and 1.3590(201) are observed and they are in accordance with the ZnO (International Center for Diffraction Data, JCPDS 5-0664). No peaks of impurity are observed, suggesting that the high purity ZnO was obtained. In addition, the peak is widened implying that the particle size is very small according to the Debye-Scherrer formula<sup>26</sup>:

$$D = \frac{K\lambda}{B \cos \theta}$$

where K is the Scherrer constant taken as 0.94,  $\lambda$  the X-ray wavelength ( $\text{CuK}\alpha = 0.15406 \text{ nm}$ ), B the peak width of half-maximum and  $\theta$  is the Bragg diffraction angle. The average crystallite size D is  $41 \pm 1 \text{ nm}$  calculated using the Debye-Scherrer formula.

**Dielectric permittivity study:** The dielectric parameter as a function of frequency is described by the complex permittivity

$$(\omega)^* = (\omega)' - (\omega)'' \quad (1)$$

where the real part  $\epsilon'$  and imaginary part  $\epsilon''$  are the components for the energy storage and energy loss, respectively, in each cycle of the electric field. The measured capacitance, C was used to calculate the dielectric constant,  $\epsilon'$  using the following expression.

$$\epsilon' = \frac{Cd}{\epsilon_0 A} \quad (2)$$

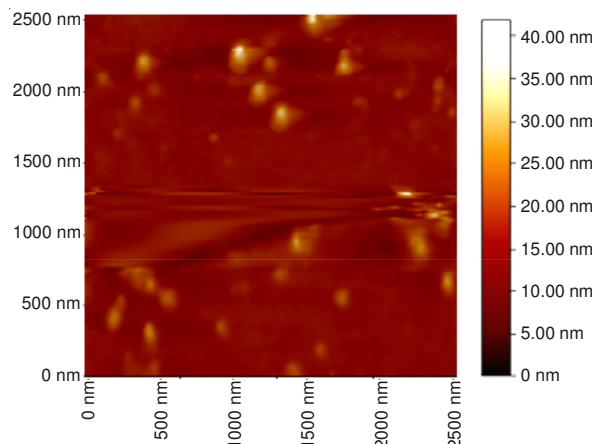


Fig. 2. (a) Represent the AFM 2-D image with maximum high (40 nm) of the ZnO nanoparticles

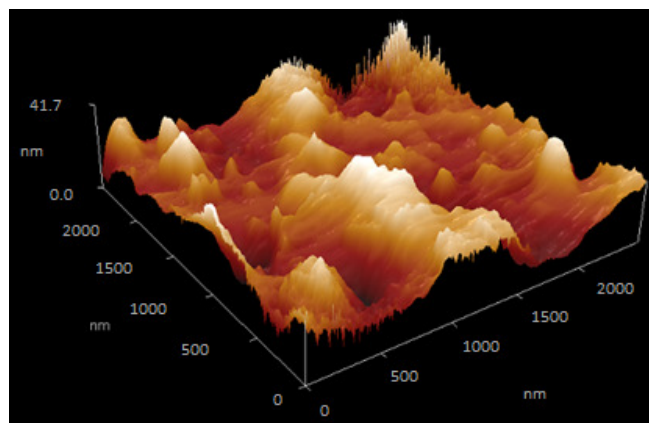


Fig. 2. (b) Represent the AFM 3-D image with maximum high (40.7 nm) of the ZnO nanoparticles

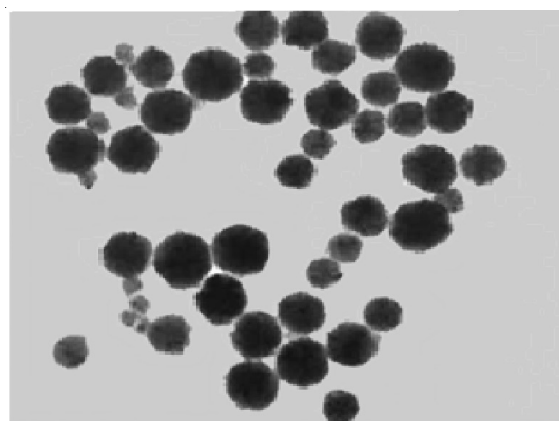


Fig. 2. (c) Represent the scanning electron micrographs of the synthesized ZnO nanoparticles

where d is the thickness between the two electrodes, A is the area of the electrodes,  $\epsilon_0$  is permittivity of the free space,  $\epsilon_0 = 8.85 \times 10^{-12} \text{ F/m}$  and  $\omega$  is the angular frequency;

$$\omega = 2\pi f \quad (3)$$

f is applied frequency, where d is sample thickness and A is surface area of the sample.

Whereas for dielectric loss<sup>27</sup>,  $\epsilon''(\omega)$  and  $\tan \delta$ :

$$(\omega)'' = (\omega)' \tan \delta (\omega) \quad (4)$$

The electric modulus is the reciprocal of the permittivity in complex form<sup>31</sup> was found using eqn. 5:

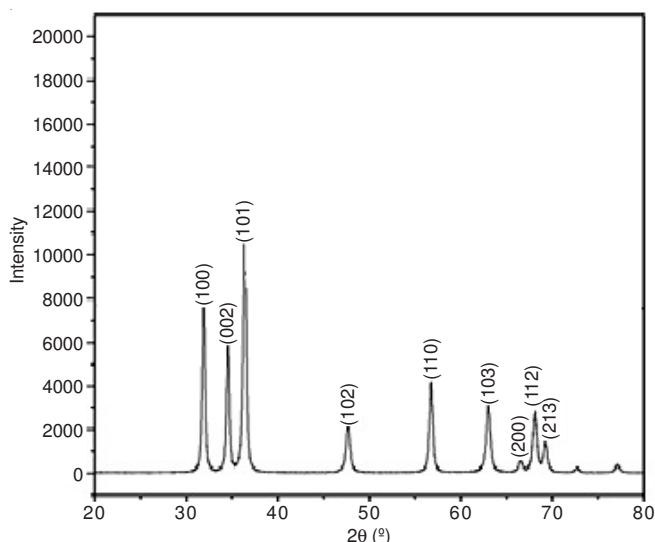


Fig. 3. XRD pattern of ZnO nanoparticles powder

$$M^* = \frac{1}{\epsilon^*} = M' + M'' \quad (5)$$

where  $M'$  and  $M''$  are the real and imaginary part of dielectric modulus and was calculated by eqns. 6 and 7:

$$M' = \frac{\epsilon'}{\epsilon'^2 + \epsilon''^2} \quad (6)$$

$$M'' = \frac{\epsilon''}{\epsilon'^2 + \epsilon''^2} \quad (7)$$

From the imaginary part of electrical modulus,  $M''$ , the relaxation time  $t$  of the orientation of dipoles can be obtained. The peak for angular frequency, ( $\omega$ ) can be obtained from the graph  $M''$  versus  $\log$  frequency<sup>27</sup>.

$$\tau = \frac{1}{\omega'} \quad (8)$$

In Fig. 4 the real permittivity slope variations with respect to frequency can be considered to be very minimal since the nanocomposite permittivity slope is almost the same as that of pure of PVA-acetal composite polymer films in frequency rang more than  $3.5 \times 10^3$  Hz, but at frequencies less than  $3.5 \times 10^3$  Hz, there is a noticeable change in the permittivity slope, this observation of the steepness in the permittivity slope at frequencies lower than  $3.5 \times 10^3$  Hz is due to the influence of ZnO filler nanoparticles.

The dielectric properties of materials are mainly determined by their polarizabilities at a given frequency. For multicomponent systems, when free charge carriers migrate through the material, space charges build up at the interfaces of the constituents owing to the mismatch of the conductivities and dielectric constants of the materials at the interfaces. This is called interfacial polarization. The interfacial polarization in polymers having structural inhomogeneities (e.g., nanoparticles) can be identified by low-frequency ( $10^2$ - $10^5$  Hz) dielectric measurement based on Maxwell-Wagner-Sillar's polarization<sup>28</sup> and the changes in the permittivity values as a function of frequency are attributed to dielectric relaxations. These are more pronounced at low frequencies due to micro-Brownian motion of the whole chain (segmental movement), which

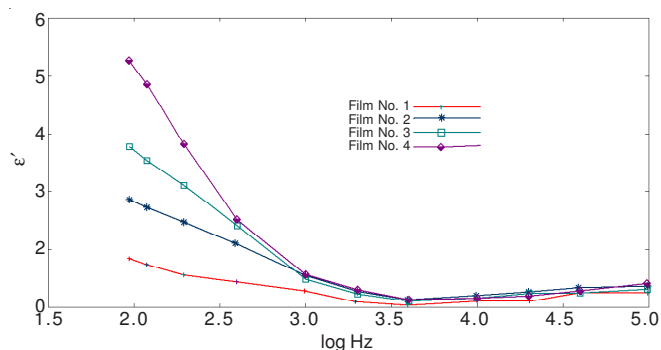


Fig. 4. Relative permittivity of PVA-poly vinyl acetal composite at different concentration of ZnO nano particles

exists in heterogeneous dielectric materials and is produced by the traveling of charge carriers<sup>28</sup>. In order to study the frequency and the different concentrations of fillers dependence of relaxation processes, effective permittivity was used Figs. 4 and 5 shows the real and imaginary part of permittivity, respectively obtained through eqns. 1-3.

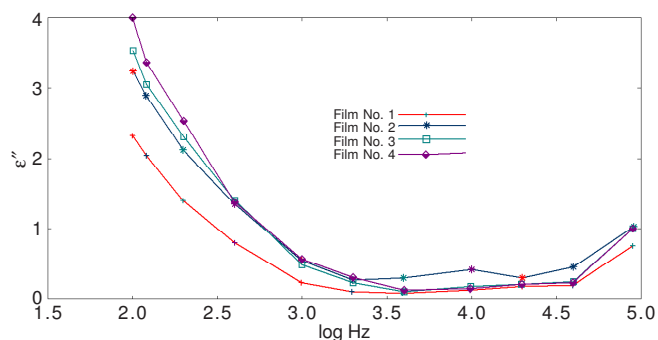


Fig. 5. Imaginary permittivity of PVA-poly vinyl acetal composite at different concentration of ZnO nano particles

The dielectric permittivity (Figs. 4 and 5) decreases with the increasing of frequency. This may be attributed to the tendency of dipoles in polymeric samples to orient themselves in the direction of the applied field. However at the frequency range ( $4 \times 10^4$ - $1 \times 10^5$ ), no decrease seems as compared for lower frequency region. This trend is observed for these graphs for different concentration of dopants. It could be explained by dipoles orientation, which difficult to rotate at high frequency range. On the other hand, the high value of  $E'$  at low frequency might be due to the electrode effect and interfacial effect of the sample<sup>29</sup>. Moreover, PVA exhibits flexible polar side groups with polar bond as the bond rotating having intense dielectric transition. and the electrical modulus was used. Figs. 6 and 7 show the real and imaginary parts of the electrical modulus, respectively obtained through eqns. 5-7 as a function of frequency<sup>30</sup>. The value at frequency region (below  $4 \times 10^3$  Hz for real modulus and  $0.4 \times 10^3$  Hz for imaginary modulus) indicates the removal of electrode polarization and the two figures show the calculated value of real and imaginary part of electrical modulus, respectively for composite films at different concentration of dopants. In Fig. 7 the peaks were shifted-up to higher frequency with the increasing of ZnO nanoparticles concentrations, it also shows that the height of the peaks proportional to the ZnO nanoparticles concentration and as relaxation time decreases. Note that the frequency



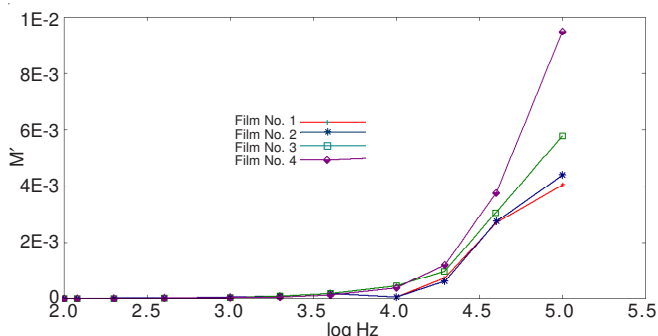


Fig. 6. Real dielectric modulus of PVA-poly acetal composite at different concentration of ZnO nano particles

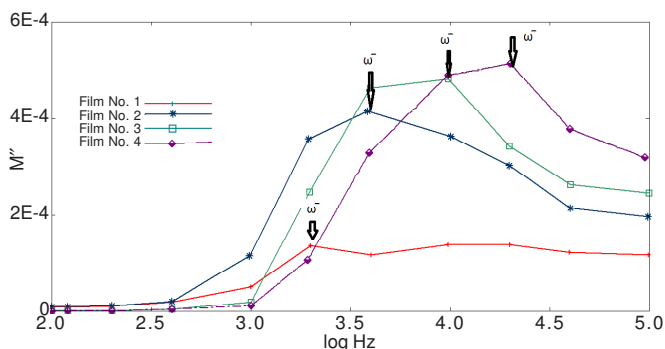


Fig. 7. Imaginary dielectric modulus of PVA-acetal composite polymer films at different ZnO nanoparticles

at the maximum of the peak of  $M''$  show the  $(\omega')$  the relaxation frequency,  $(\omega'')$  as tabulated in the inset Fig. 7). Table-2 shows the relaxation time,  $\tau$  for poly(vinyl acetal)/PVA composite doped with ZnO nanoparticles at different concentration of the dopants. The relaxation times were obtained (eqn. 8). From the whole data, one can conclude that with the increasing amount of the ZnO nanoparticles, the relaxation time is relatively reduced. These results confirm the explanation for the dielectric constant and dielectric loss characteristics as relaxation times decreases with the increasing composition of the ZnO nanoparticles, which were effected on interfacial polarization, since relaxation processes were influenced by the interfacial polarization effect which generated electric charge accumulation around the ZnO nanoparticles and the displacement of peak as the particle content increased and this is identify with work of Tsangaris *et al.*<sup>31</sup>.

TABLE-2

RELAXATION TIME,  $\tau$  FOR POLY 4-METHYL BENZYLEDENE VINYL ALCOHOL-PVA COMPOSITE POLYMER WITH ZnO NANOPARTICLES FILMS

Film No.	ZnO concentration (%)	$\tau$ relaxation time (Hz)
1	0.0	$1.28 \times 10^{-8}$
2	1.71	$7.81 \times 10^{-9}$
3	2.81	$1.75 \times 10^{-8}$
4	3.79	$1.33 \times 10^{-8}$

## Conclusion

The results show that the poly 4-methyl benzyledene vinyl alcohol/PVA composite polymer films have both electric and

electronic properties. The composite polymer films exhibit the combination of intrinsic dielectric anisotropy as a result of the competition of free charges. Relaxation times become shorter as the composition of ZnO nanoparticles is increased indicates that multiple path of the system to be relaxed due to high availability of free charges.

## REFERENCES

- H. Althues, J. Henle and S. Kaskel, *Chem. Soc. Rev.*, **36**, 1454 (2007).
- M. Kozako, R. Kido, N. Fuse, Y. Ohki, T. Okamoto and T. Tanaka, *IEEE Conf. Electr. Insul. Dielectr. Phenomena*, pp. 398-401 (2004).
- B.J. Ash, R.W. Siegel and L.S. Schadler, *J. Polym. Sci. B*, **42**, 4371 (2004).
- D. Ma, Y.A. Akpalu, Y. Li, R.W. Siegel and L.S. Schadler, *J. Polym. Sci. B, Polym. Phys.*, **43**, 463 (2005).
- J.K. Nelson, J.C. Fothergill, L.A. Dissado and W. Peasgood, *IEEE Proceedings of the Conference on Elec Insul & Dielec Phenomena, Mexico*, pp. 295-298 (2002).
- G.C. Montanari, D. Fabiani, F. Palmieri, D. Kaempfer, R. Thomann and R. Mulhaupt, *IEEE Trans. Dielectr. Electr. Insul.*, **11**, 754 (2004).
- M.F. Fréchet, *Proc. 35th Sympos, Electrical Electronics Insulating Materials and Applications in Systems, Tokyo, Japan*, pp. 25-32 (2004).
- T. Ramanathan, S. Stankovich, D.A. Dikin, H. Liu, H. Shen and S.T. Nguyen, *J. Polym. Sci. B, Polym. Phys.*, **45**, 2097 (2007).
- L. Vaisman, E. Wachtel, H.D. Wagner and G. Marom, *Polymer*, **48**, 6843 (2007).
- A. Okada and A. Usuki, *Macromol. Mater. Eng.*, **291**, 1449 (2006).
- N. Moriguchi, S. Torigoe and K. Tokuchi, *Thermoplastic Polymer comPosition and Shaped Article Composed of the Same*, US Patent 2010/0273012 A1 (2010).
- D.K. Das-Gupta, *Key Eng. Mater.*, **92-93**, 1 (1994).
- D.-H. Kuo, C.-C. Chang, T.-Y. Su, W.-K. Wang and B.Y. Lin, *J. Eur. Ceramic Soc.*, **21**, 1171 (2001).
- P. Chahal, R.R. Tummala, M.G. Allen and M. Swaminathan, *IEEE Packag. Manuf. Technol.*, **21**, 184 (1998).
- P. Thomas, S. Satapathy and K. Dwarakanath, *eXPRESS Polym. Lett.*, **4**, 632 (2010).
- R. Liu, A.A. Vertegel, E.W. Bohannon, T.A. Sorenson and J.A. Switzer, *Chem. Mater.*, **13**, 508 (2001).
- R. Kaur, A.V. Singh, K. Sehrawat, N.C. Mehra and R.M. Mehra, *J. Non-Cryst. Solids*, **352**, 2565 (2006).
- J. Kubota, K. Haga, Y. Kashiwaba, H. Watanabe, B.P. Zhang and Y. Segawa, *Appl. Surf. Sci.*, **216**, 431 (2003).
- S. Singh, P. Thiyagarajan, K.M. Kant and D. Anita, *J. Appl. Phys.*, **40**, 6312 (2007).
- D.C. Reynolds, D.C. Look and B. Jogai, *J. Appl. Phys.*, **89**, 6189 (2001).
- C. Wu, X. Qiao, J. Chen, H. Wang, F. Tan and S. Li, *Mater. Lett.*, **60**, 1828 (2006).
- R. Hong, T. Pan, J. Qian and H. Li, *Chem. Eng. J.*, **119**, 71 (2006).
- J.-H. Park and S.-G. Oh, *Mater. Chem. Phys.*, **87**, 301 (2007).
- K. Nejati, Z. Rezvani and R. Pakizevand, *Int. Nano Lett.*, **1**, 75 (2011).
- I. Sakurada, *Pure Appl. Chem.*, **16**, 263 (1968).
- P. Scherrer, *Nachrichten von der Königlichen Gesellschaft der Wissenschaft zu Göttingen: Mathematisch-physikalische Klasse*, **1**, 98 (1918).
- M.H. Harun, E. Saion, A. Kassim, E. Mahmud, M.Y. Hussain and I.S. Mustafa, *J. Advancement Sci. Arts*, **1**, 1 (2009).
- C. Ku and R. Liepins, *Electrical Properties of Polymers*, Hanserp, NewYork, pp. 20-58 (1987).
- P. Dutta, S. Biswas and S.K. De, *Mater. Res. Bull.*, **37**, 193 (2002).
- L. Ramajo, M. Reboredo and M. Castro, *Composites A*, **36**, 1267 (2005).
- G. Tsangaris, N. Kouloumbi and S. Kyvelidis, *Mater. Chem. Phys.*, **44**, 245 (1996).